Issues on the Response of Existing Buildings Under Mainshock-Aftershock Seismic Sequences

J. Ruiz-García
Universidad Michoacana de San Nicolás de Hidalgo, México

SUMMARY:
This paper presents the results of examining ground motion characteristics in 92 real mainshock-aftershock earthquake ground motions recorded during the 1994 Northridge earthquakes and the 2010/2011 New Zealand earthquakes. Relevant observations of the response of structures under seismic sequences are highlighted. It is shown that the predominant period (a measure of the frequency content) of the set of mainshocks tends to be longer than that of the corresponding aftershocks. Results indicate that the inherent self-centering capability in stiffness-degrading systems is very important for constraining permanent displacements under strong aftershocks. It is also highlighted that the response of structures under artificial sequences is very different from that of real sequences, particularly when the approach of repeating the real mainshock with identical ground motion features as an artificial aftershock is employed. It is also demonstrated that the predominant period of the aftershock significantly influences the post-mainshock response.

Keywords: aftershocks, seismic sequences, residual drift demands, interstory drift demands

1. MOTIVATION

The response of structures subjected to mainshock-aftershock earthquake ground motion sequences has gained the attention from the earthquake engineering community recently, since strong aftershocks might be triggered after the mainshock. For example, after the 1994 Northridge earthquake (Mw=6.7) that affected the Los Angeles Area in California, an Mw=6.0 aftershock was felt approximately one minute later. Likewise, after the mainshock (Mw=7.0) on September 4, 2010 that struck the Canterbury region in the Southern Island of New Zealand, a strong aftershock (Mw=6.3) was felt on February 22, 2011 that hit the city of Christchurch. Hereafter, the largest aftershock is considered along with the mainshock to denote a seismic sequence. As a historical note, in the author's knowledge, Mahin (1980) carried out the first pioneering analytical study of the response of nonlinear single-degree-of-freedom (SDOF) systems subjected to mainshock-aftershock acceleration time histories recorded during the 1972 Managua earthquake. He observed that the displacement ductility demand, μ (i.e. peak inelastic displacement normalized with respect to the system's yield displacement) of elastoplastic SDOF systems slightly increased at the end of the main aftershock with respect to the mainshock. After this pioneering study, several works aimed at studying the response of structures under seismic sequences have been published in the last ten years. Some of them have been focused on the nonlinear response of SDOF systems (e.g. Amadio et al. 2003, Hatzigeorgiou and Beskos 2009), while others have focused their attention in the response of multiple-degree-of-freedom (MDOF) systems (e.g. Lee and Foutch 2004, Li and Ellingwood 2007, Hatzigeorgiou and Liolios 2010, Ruiz-García and Negrete-Manriquez, 2011). Most of the previous studies employed artificial seismic sequences instead of real (i.e. as-recorded) mainshock-aftershocks sequences to evaluate the structural seismic response. They employed artificial sequences using the mainshock acceleration time-history as a seed for simulating the following aftershocks using the following approaches: 1) back-to back, or repeated, approach (e.g. Amadio et al. 2003, Lee and Foutch 2004, Li and Ellingwood

2007, Hatzigeorgiou and Beskos 2009); or 2) randomized approach (e.g. Li and Ellingwood 2007, Hatzigeorgiou and Liolios 2010). The first approach consists on repeating the real mainshock, at scaled or identical amplitude, as an artificial aftershock, which assumes that the ground motion features such as frequency content and strong motion duration of the mainshock and aftershock(s) are the same. Lee and Foutch (2004), and Li and Ellingwood (2007) made an effort of taking into account the aftershock hazard level by scaling down the amplitude of the second ground motion. However, as explained above, this seismic scenario is unrealistic since the mainshock and the largest aftershock are related to different asperity areas and, as a consequence, they have different frequency content. The second approach consists on ensemble a set of real mainshocks, and generating artificial sequences by selecting a mainshock and simulating the remaining aftershocks by repeating the mainshock waveformat repeatedly, at reduced or identical amplitude, with no change in spectral content as an artificial aftershock.

It should be noted that although most of the previous studies developed extensive analytical studies and provided information on the effect of seismic sequences on the response of structures, the use of artificial seismic sequences, either generated from the repeated or the randomized approach, could lead to misunderstand the response of structures under real seismic sequences. This situation might occur if the relationships of the ground motion characteristics between the mainshock and the following aftershocks are not properly represented in the artificial sequences. Therefore, the main objectives of the investigation reported in this paper were three-fold: a) to characterize the ground motion features (i.e. amplitude, frequency content, and strong-motion duration) of 92 mainshock-largest aftershock ground motion sequences recorded during the 1994 Northridge earthquakes in the United States and the 2010/2011 Canterbury earthquakes in New Zealand, b) to identify the relationships between the ground motion features of recorded mainshock-aftershocks, and c) to investigate the impact of the frequency content relationship between the mainshock-aftershock in the dynamic response of frame buildings.

2. EARTHQUAKE GROUND MOTIONS AND EXISTING STEEL FRAMES CONSIDERED IN THIS STUDY

2.1. Set of Mainshock-Aftershock Seismic Sequences

In this study, a set of mainshock and its corresponding largest aftershock ground motions (hereafter denoted as a seismic sequence) recorded from the 1994 Northridge earthquake was assembled from the Pacific Earthquake Engineering (PEER) database (PEER, 2011). Seismic sequences were selected according with the following criteria: a) magnitude of main aftershock event equal to or greater than 4.0; b) available information about the soil condition, which correspond to Soil Type A, B, C or D (i.e. bedrock and stiff soils); c) acceleration time histories recoded on stations placed on free field or low-height buildings were soil-structure interaction effects were negligible; and d) seismic sequences having peak ground acceleration (PGA) of the mainshock horizontal component greater than 100 cm/s^2 and PGA of the aftershocks greater than 50 cm/s^2. Under these criteria 58 seismic sequences from two orthogonal horizontal components were selected for this investigation. It should be noted that 14 out of 58 seismic sequences correspond to mainshock ground motions having near-fault features. For example, seismic sequences recorded at Rinaldi Receiving Station and Sylmar Converter Station were considered in this study as shown in Fig. 2.1. Detailed information of the selected seismic sequences can be found in Ruiz-García and Negrete-Manriquez (2011). In addition, a second set of 34 seismic sequences were identified from the September 4, 2010 Darfield earthquake and the February 22, 2011 Christchurch earthquake that struck the Canterbury region in the Southern Island of New Zealand. The EQGM's were gathered from the Center for Engineering Strong Motion Data (CESMD 2012). Unlike typical mainshock-aftershock sequences, some stations recorded greater peak ground accelerations (PGA) due to the aftershock than those from the mainshock as illustrated in Fig. 2.1. This situation can be explained since some accelerographics stations were located at a shorter epicentral distance from the aftershock epicenter than that from the mainshock epicenter. This is an unusual seismic scenario that design seismic codes do not take into account nowadays.

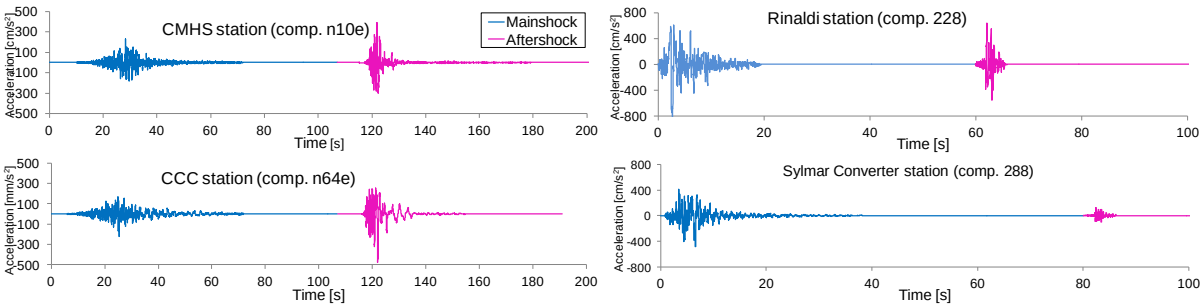

Figure 2.1. Examples of seismic sequences considered in this study from the 2010/2011 New Zealand earthquakes (left figures) and the 1994 Northridge earthquakes (right figures)

2.2. Building Frame Models

In order to gain insight about the displacement time-history response of typical New Zealand building frames, the response of an equivalent single-degree-of-freedom (E-SDOF) systems representative of a 5-story reinforced concrete frame under selected seismic sequences was computed in the first stage of this study. In addition, three regular three-bay frame models having three different number of stories (N=4, 8, and 12), which are representative of exterior steel moment resisting frames found in typical low-to-medium height-rise existing steel office buildings, were subjected to the 1994 Northridge sequences. It should be mentioned that all frames have uniform mass distribution and a non-uniform lateral stiffness distribution over the height. The frame models were originally designed by Santa-Ana and Miranda (2000) using the lateral load distribution specified in the 1997 Uniform Building Code for a structure located in Zone 4 on soil type S1 (i.e. a soil profile with either a rock-like material or stiff or dense soil). he frames were modeled as two-dimensional centerline models using the computer program RUAUMOKO (Carr, 2008). Rayleigh damping equal to 5% of critical was assigned to the first and second modes for all the frame models. During the analysis, local P -delta effects were included (i.e. large displacement analysis). Beams and columns were modeled as frame elements which concentrate their inelastic response in plastic hinges located at their ends. While a non-degrading elasto-plastic moment-curvature relationship that considers *axial-flexural bending* interaction was considered to model the hysteretic behavior of the steel columns, an elasto-plastic moment-curvature relationship that includes strength degradation due to fracture, was considered for the steel beams. Flexural moment capacity for beams and columns was determined using actual yield strength capacity of 49 and 58 ksi, respectively. From modal and nonlinear static analyses, main dynamic properties were obtained and summarized in Table 2.1.

Table 2.1. Fundamental Period of Vibration, T_1, Roof Yield Displacement, $\delta_{y,roof}$, Yield Strength Coefficient, C_y, and Normalized Modal Participation Factor, $\Gamma_1\phi_{1,roof}$, Obtained for Each Generic Frame

N	T_1 [sec]	$\delta_{y,roof}$ [cm]	C_y	$\Gamma_1\phi_{1,roof}$
4	1.23	16.0	0.32	1.22
8	1.92	36.0	0.25	1.31
12	2.61	47.0	0.18	1.31

3. ISSUES REGARDING THE SEISMIC RESPONSE UNDER MAINSHOCK-AFTERSHOCK SEQUENCES

3.1. Frequency Content Characteristics of the Mainshock and Corresponding Aftershock

In order to study whether the main aftershock acceleration time-histories have similar frequency content than their corresponding mainshock time-histories, the predominant period of the ground motion, T_g, and the bandwidth, Ω, was used as a measure the frequency content. Both frequency measures were derived from the elastic velocity spectra. The predominant period of the ground motion was defined as the period at which the maximum ordinate of a five percent damped relative velocity

spectrum occurs. An analogue measure of the ground motion spread about the central period, or bandwidth, as a function of the spectral parameters computed from the square velocity spectra was also computed, which allows defining whether a ground motion has narrowband or broadband frequency content around its central frequency or central period. Following the aforementioned definitions, the relationship between T_g and Ω for all ordinary mainshock and main-aftershock ground motions is shown in Figs. 3.1a, 3.2a, and 3.3a. From Figs. 3.1a and 3.2a, it can be observed that the predominant period of the mainshocks tends to be longer than that of the aftershocks for the Northridge earthquakes. The relationship between the predominant period of the ground motion corresponding to the mainshock and main-aftershock is also shown in Figs. 3.1b, 3.2b, and 3.3b. For these seismic scenarios, it was found that mainshock ground motions from the 1994 Northridge earthquake have predominant periods longer than those of their largest aftershock ground motions in 93% of the sequences, while this happened in 65% of the New Zealand sequences. The sample correlation coefficient reported for each set lead to the conclusion that the predominant period of the mainshocks is weakly linear correlated, from a statistical point of view, with the predominant period of the main-aftershocks. A similar examination employing additional seismic sequences recorded worldwide lead to the conclusion that the simulation approach of repeating mainshock as aftershock is not appropriate (Ruiz-García 2012).

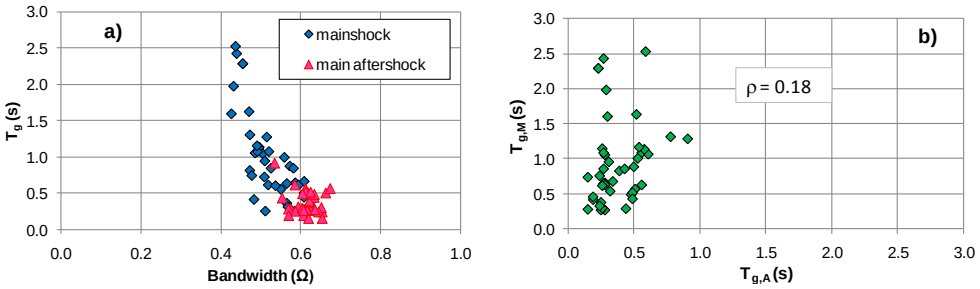

Figure 3.1. Ordinary ground motions from the 1994 Northridge earthquakes: a) relationship T_g between Ω for mainshock and aftershocks, b) relationship of T_g for mainshock and T_g for aftershocks

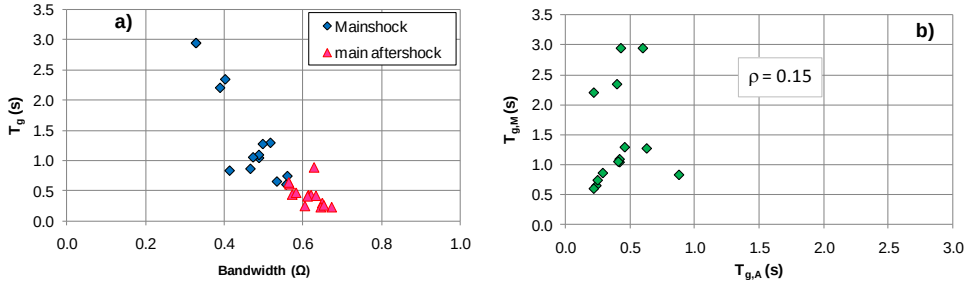

Figure 3.2. Near-fault ground motions from the 1994 Northridge earthquakes: a) relationship T_g between Ω for mainshock and aftershocks, b) relationship of T_g for mainshock and T_g for aftershocks

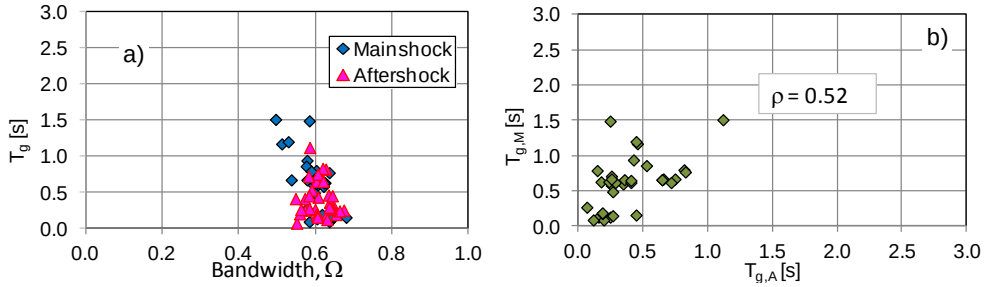

Figure 3.3. Ground motions from the 2010/2011 New Zealand earthquakes: a) relationship T_g between Ω for mainshock and aftershocks, b) relationship of T_g for mainshock and T_g for aftershocks

3.2. Effect of Hysteretic Behaviour

Figure 3.4 illustrates the response of the E-SDOF system under the seismic sequences recorded in Stations CMHS, CHHC, CCCC, and CBGS taking into account two types of hysteretic behaviour: Elastoplastic (EPP) and Modified-Clough (MC). The hysteretic behavior assuming a MC model is also presented next to each displacement time-history response. From the figure, it can be seen that the behavior of the E-SDOF systems remain nearly elastic, with small permanent displacements at the end of the mainshock of September 4, 2010. However, it can clearly be seen that the aftershock of February 22, 2011 triggers larger displacement response than that of the mainshock, both in terms of peak and permanent displacement demand. It should be noted that peak displacement demands are larger in the presence of stiffness degradation than when elastoplastic behavior is considered. However, an interesting observation is that the stiffness-degrading behavior (i.e. MC model) leads to smaller permanent displacements due to a inherent self-celtering capability in the hysteretic loops that constraints permanent displacement. Furthermore, it was found that the this self-centering capability is a more important factor in limiting permanent displacements than the post-yield stiffness ratio (e.g. comparing the displacement response with 5% and nearly 0% post-yield stiffness ratio).

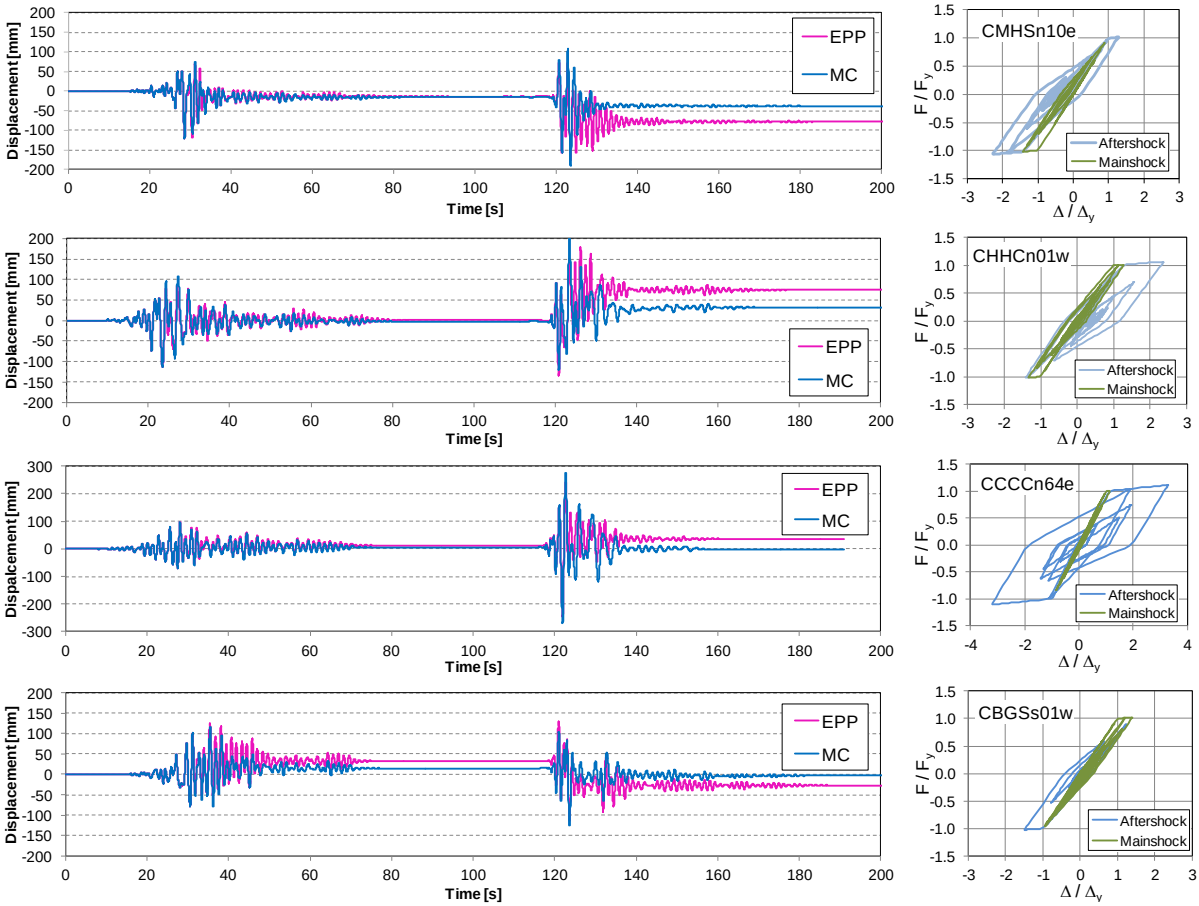

Figure 3.4. Displacement time-history response and hysteretic behavior of an E-SDOF system representative of a 5-story RC building under 4 sequences recorded in Christchurch city

3.3. Effect of Frequency Content

It is of particular interest to further investigate the effect of the frequency content of the aftershock in the building response. However, all the near-fault aftershocks in the ground motion database have T_g's shorter than the building's fundamental period of vibration. Then, artificial aftershocks having different frequency content (i.e. pulse period) were generated through a velocity pulse model explained in Ruiz-García and Negrete-Manriquez (2011). For example, Fig. 3.5a illustrates the

recorded aftershock ground velocity and acceleration time-history recorded at Rinaldi Receiving station and the fitted velocity pulse model. Using the as-recorded mainshock and the acceleration time-history with acceleration time-history obtained from the velocity pulse model, it was first verified that this artificial sequence could reproduce the displacement time-history obtained from the real sequence. Next, the velocity pulse model was calibrated to have different pulse periods (i.e. frequency content) while keeping the same peak ground acceleration of the as-recorded aftershock. The displacement time-history recorded in the first story of the 4-story frame model when subjected to as-recorded mainshock-pulse type aftershocks sequences is shown in Fig. 3.5b. From the figure, it can clearly be observed the effect of the aftershock frequency content in permanent displacements at the end of the sequence.

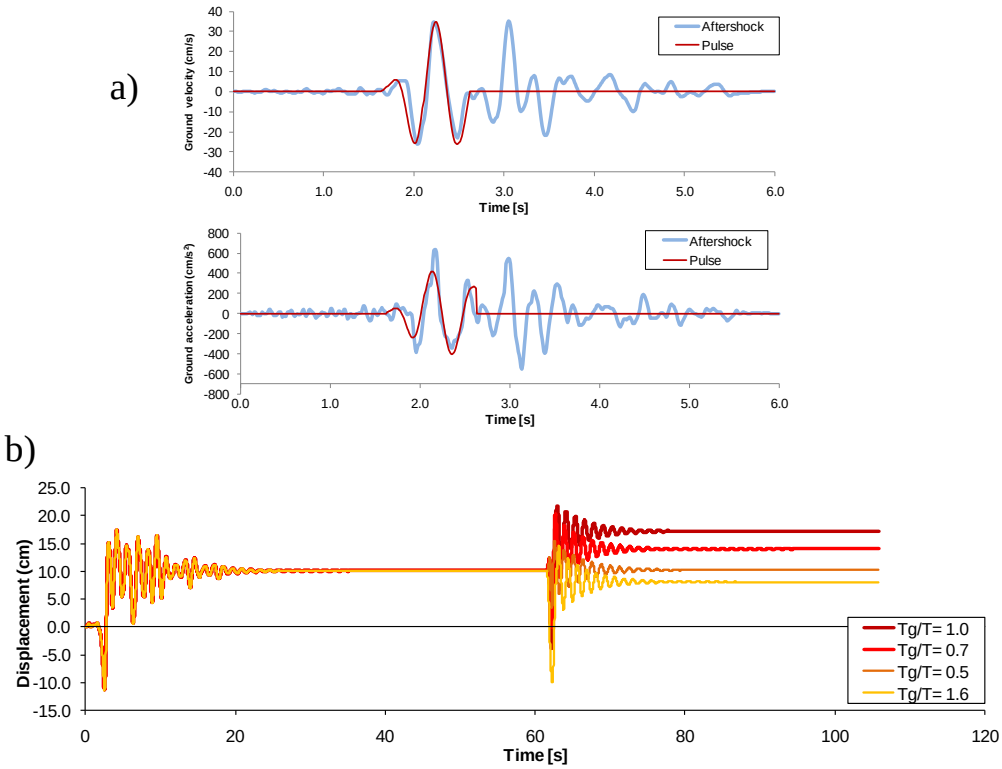

Figure 3.5. a) Comparison of as-recorded ground velocity and acceleration of main-aftershock recorded at Rinaldi Receiving station with a pulse model, b) Displacement time-history response of the 4-story frame model under as-recorded mainshock and artificial sequences having pulse-type aftershocks.

3.4. Effect of Artificial Seismic Sequences vs. Real Seismic Sequences

It should be recognized that previous results, mainly for peak inter-story drift demand, are opposite to some of the prior studies. However, most of the preceding studies employed artificial seismic sequences, either from a repeated or randomized approach. As shown in the previous section, the repeated and randomized approach could lead to the conclusion that aftershocks consistently increase peak and permanent displacement demands from the mainshock. Therefore, it is of interest to examine the response of frame models under as-recorded and artificial seismic sequences and to investigate the level of overestimation in drift demands that artificial seismic sequences generated from the repeated and randomized approach induces to the frames.

For this purpose, let's consider the as-recorded mainshock-aftershock acceleration time-history (component 228) recorded in the Rinaldi Receiving Station during the 1994 Northridge earthquake. This seismic sequence is chosen since the main aftershock has the largest PGA among the recorded aftershocks in the catalogue and it has a $(\mathrm{PGA})_{\mathrm{M}}/(\mathrm{PGA})_{\mathrm{A}}$ ratio equal to 0.79 (see Fig. 2.1). In addition, artificial seismic sequences are generated by repeating the mainshock as the aftershock (i.e.

back-to-back case) and using the mainshock acceleration time-history recorded in Sylmar Converter station as an aftershock (i.e. randomized case). Fig. 3.6 shows the as-recorded and artificial seismic sequences. It can clearly be seen that the artificial seismic sequences have very different ground motion features than the as-recorded seismic sequence.

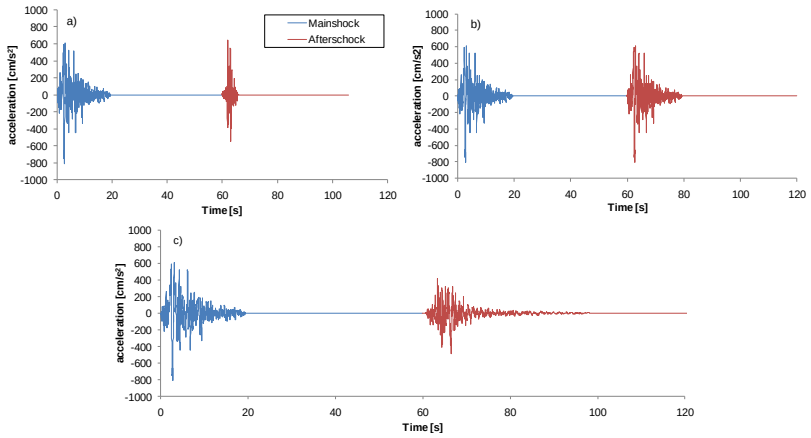

Figure 3.6. Seismic sequences in the near-fault environment (Rinaldi Receiving station, comp. 228): a) as-recorded; b) back-to-back case; c) randomized case.

Therefore, each frame was subjected to the as-recorded seismic sequence and the two artificial sequences. For instance, the displacement time-history obtained from the first story of the 4- and 12-story frame models is shown in Figs. 3.7 and 3.8, respectively. From the figures, it can be seen the mainshock triggers permanent displacement at the end of the excitation in both frames, mainly in the 4-story frame. This observation could be explained since the calculated predominant period the mainshock ground motion is 1.05s, which is close than the first-mode period of vibration of the 4-story frame (T_1=1.23 s, T_g/T_1=0.85). However, the as-recorded aftershock does not increase either peak and permanent displacement demands in both frames, which might be explained since the predominant period of the aftershock (T_g=0.41s, T_g/T_1=0.33) is shorter than either the fundamental period of vibration of both frames (i.e. undamaged state at the end of the mainshock) or the period of vibration of the damaged frames. On the other hand, it should be noted that artificial seismic sequences lead to larger permanent displacements of each frame at the end of the artificial aftershock than the as-recorded sequence. In both cases, the artificial sequence defined by the back-to-back approach leads to the largest permanent displacement.

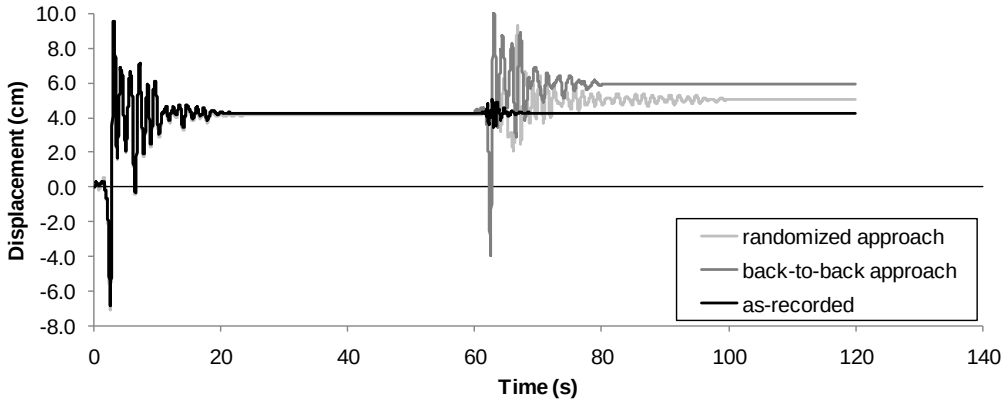

Figure 3.7. Displacement time-history response of a 4-story frame model under as-recorded and artificial seismic sequences from the Rinaldi Receiving station (comp. 228)

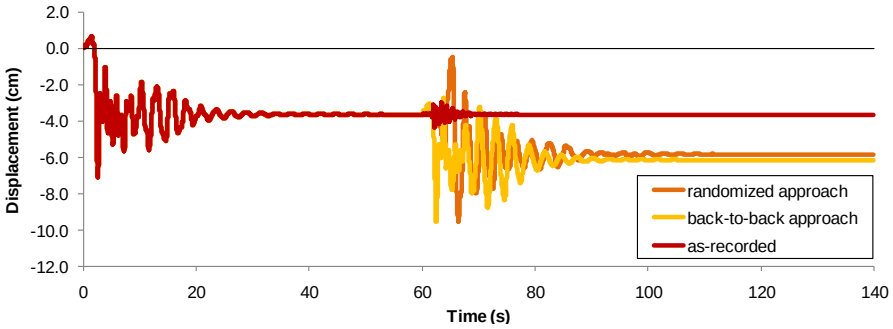

Figure 3.8. Displacement time-history response of a 12-story frame model under as-recorded and artificial seismic sequences from the Rinaldi Receiving station (comp. 228)

Fig. 3.9 shows a comparison of the height-wise distribution of IDR for all frames computed from the as-recorded and artificial near-fault seismic sequences. Results are presented in terms of mean-plus-one-standard deviation in order to include the record-to-record variability. As can be expected, it can be seen that artificial sequences trigger larger maximum IDR over all stories, while the level of overestimation of IDR depends on the specific story and the period of vibration of the frame. For instance, IDR's in the first story of each frame computed from the repeated approach are larger about 13%, 24% and 35% than the corresponding IDR's calculated from as-recorded sequences.

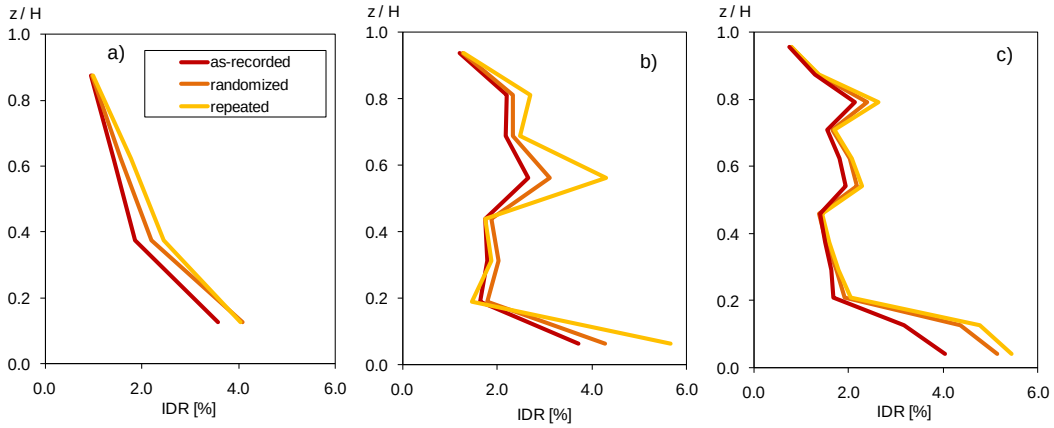

Figure 3.9. Height-wise distribution of mean-plus-one-standard deviation peak (transient) inter-story drift demand under as-recorded and artificial near-fault seismic sequences: a) 4-story frame; b) 8-story frame; and c) 12-story frame.

An important finding for probabilistic assessment of buildings under a mainshock-aftershock scenario is that the record-to-record variability, measured by the logarithmic standard deviation of IDR, computed from the artificial sequences is, in general, larger than that computed from the as-recorded sequences. For example, height-wise distribution of logarithmic standard deviation of IDR computed from the near-fault sequences is shown in Fig. 3.10. This observation has impact while computing fragility curves of peak interstory drift demands and, as a consequence, in seismic hazard curves of peak-interstory drift demand.

A comparison of IDR's triggered by as-recorded and artificial (repeated) far-field seismic sequences is illustrated in Fig. 3.11. Under this seismic environment, the artificial mainshock-aftershock sequences do not trigger significantly different mean-plus-one-standard deviation IDR's than the as-recorded seismic sequences. For example, IDR's in the first story computed from the repeated approach are larger about 13%, 33% and 6% than the corresponding IDR's calculated from as-recorded sequences. Finally, a comparison of mean-plus-one-standard deviation IDR's computed from as-recorded and artificial (repeated) near-fault sequences is shown in Fig. 3.12. It can clearly be seen that the use of artificial seismic sequences tends to overestimate the amplitude of residual drift demands. The level of overestimation depends on the number of stories and the story height.

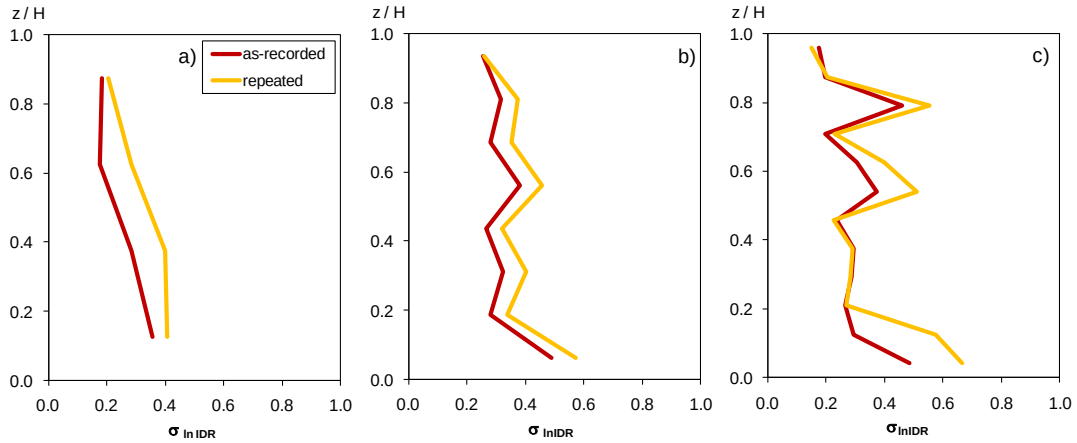

Figure 3.10. Height-wise distribution of log standard deviation of peak (transient) inter-story drift demand under as-recorded and artificial (repeated approach) near-fault seismic sequences: a) 4-story frame; b) 8-story frame; and c) 12-story frame.

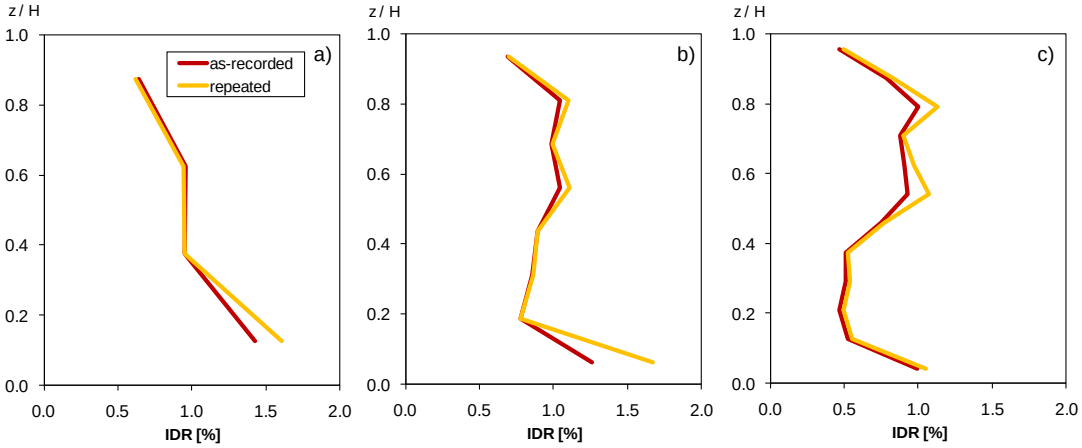

Figure 3.11. Height-wise distribution of mean plus one standard deviation of peak (transient) inter-story drift demand under as-recorded and artificial (repeated approach) far-field seismic sequences: a) 4-story frame; b) 8-story frame; and c) 12-story frame.

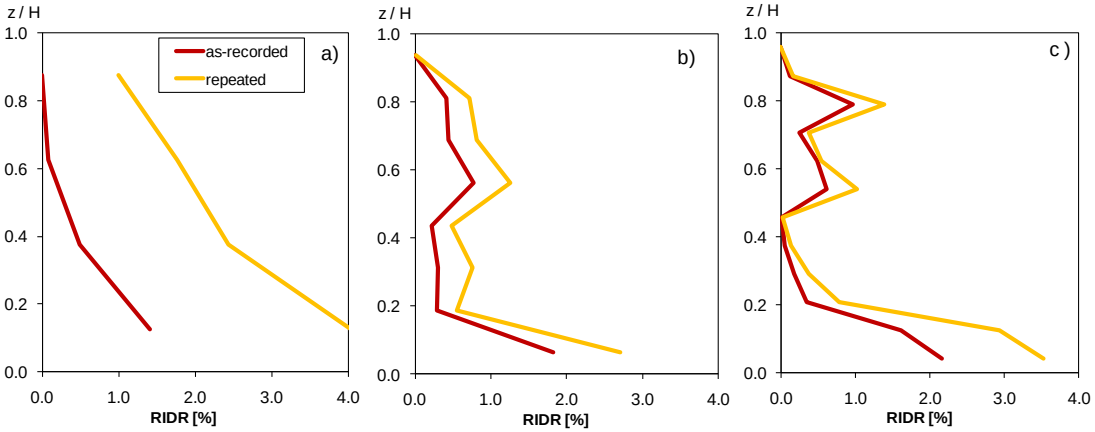

Figure 3.12. Height-wise distribution of mean plus one standard deviation of residual (permanent) inter-story drift demand under as-recorded and artificial (repeated approach) near-fault seismic sequences: a) 4-story frame; b) 8-story frame; and b) 12-story frame.

5. CONCLUSIONS

From the results of this investigation, the following conclusions are drawn:

- The frequency content, measured by the predominant period of the ground motion and bandwidth, of the mainshock and the main aftershock of the seismic sequences considered in this investigation are weakly correlated (from a statistical point of view). Thus, there is no evidence that support simulating seismic sequences using the mainshock as seed for reproducing the aftershock (i.e. seismic sequences simulated as back-to-back mainshocks).
- From the response of an equivalent single-degree-of-freedom system representative of a 5-story RC building subjected to the 2010/2011 New Zealand sequence, it was found that the inherent self-centering capability of stiffness degrading systems constrained permanent displacements triggered by the aftershock on February 22, 2011. It was also found that this capability is more important in limiting permanent displacements than the post-yield stiffness ratio.
- Unlike previous results based on artificial seismic sequences, it was found that as-recorded aftershocks do not significantly increase peak and permanent drift demands of existing steel frames, which is particularly true for the seismic sequences recorded during the 1994 Northridge earthquake. This observation can be explained since the frequency content of the aftershock is shorter, and in some cases much smaller, that the frequency of the structure at the end of the mainshock.
- Artificial seismic sequences lead to overestimation of the maximum lateral drift demands as well as to the record-to-record variability. The level of overestimation depends on the approach for developing artificial sequences (repeated or randomized approach).

AKCNOWLEDGEMENTS

The author would like to express his gratitude to *Universidad Michoacana de San Nicolás de Hidalgo* and *The National Council for Science and Technology* (CONACYT) in México for the financial support provided to develop the research reported in this paper. In addition, the author would like to thanks former research assistant Juan C. Negrete for their contribution to this work.

REFERENCES

Amadio, C., Fragiacomo, M., Rajgelj, S. (2003). The Effects of repeated earthquake ground motions on the non-linear response of SDOF systems. *Earthquake Engineering and Structural Dynamics*. **32**:291-308.

Carr, A.J. (2008). RUAUMOKO-Inelastic Dynamic Analysis Program. User's manual, Dept. of Civil Engineering, University of Canterbury, Christchurch, New Zealand.

CESMD (2012). Center for Engineering Strong Motion Data. http://www.strongmotioncenter.org/. Last access: 03/21/12

Lee, K., Foutch, D.A. (2004). Performance evaluation of damaged steel frame buildings subjected to seismic loads. *Journal of Structural Engineering.* **130:4**, 588-599.

Li, Q., Ellingwood, B.R. (2007). Performance evaluation and damage assessment of steel frame buildings under main shock-aftershock sequences. *Earthquake Engineering and Structural Dynamics.* **36**, 405-427.

Hatzigeorgiou, G.D., Beskos, D.E. (2009). Inelastic displacement ratios for SDOF structures subjected to repeated earthquakes. *Engineering Structures*. **31:11**, 2744-2755.

Hatzigeorgiou, G.D., Liolios, A.A. (2010). Nonlinear behaviour of RC frames under repeated strong ground motions. *Soil Dynamics and Earthquake Engineering*. **30**:1010–25.

Mahin, S.A. (1980). Effects of duration and aftershocks on inelastic design earthquakes. *Seventh World Conference on Earthquake Engineering*. **Vol. 5:** 677-679.

PEER (2011) Pacific Earthquake Engineering Research Center PEER Strong Motion Database. www/http://peer.berkeley.edu/nga/. Last access: 12/06/2011.

Ruiz-García, J. (2012). Mainshock-aftershock ground motion features and their influence in building's seismic response. *Journal of Earthquake Engineering*. **16:5**, 719-737.

Ruiz-García, J., Negrete-Manriquez, J.C. (2011). Evaluation of drift demands in existing steel frames under as-ecorded far-field and near-fault mainshock–aftershock seismic sequences. *Engineering Structures.* **33:2**, 621-634.

Santa-Ana, P.R., Miranda, E. (2000). Strength-reduction factors for multi-degree-of-freedom systems. *Twelfth World Conf. on Earth. Engrg*., Auckland, Paper 1446.

Uma SR, Ryu H, Luco N, Liel AB, Raghunandan M (2011) Comparison of main-shock and aftershock fragility curves developed for New Zealand and US buildings. *Ninth Pacific Conference on Earthquake Engineering Building an Earthquake-Resilient Society*. Paper No. 227.